SYNTHESIS AND COMPOSITION CHARACTERIZATION OF $K_{0.5}Na_{0.5}NbO_3$–$KSr_2Nb_5O_{15}$ CERAMICS

#LIANGLIANG LIU, ZHUANGZHUANG GUO, YONGQIANG WANG, HAIWEI JIANG

College of Materials Science and Engineering, Taiyuan University of Technology, Taiyuan 030024, PR China

#E-mail: liuliangliang_2004@163.com

Keywords: $KSr_2Nb_5O_{15}$, Ferroelectric ceramics, Microstructure, Dielectric property

$KSr_2Nb_5O_{15}$ modified potassium sodium niobate ceramics ($(1 – x)KNN–xKSN$) were fabricated by a pressure-less solid-state method, using Bi as a sintering aid. Synthesis and composition characterization of the $(1 – x)KNN–xKSN$ ceramics were investigated. It was found that the KSN addition was favorable to the densification of the $(1 – x)KNN–xKSN$ ceramics due to the improvement of sintering temperature and the absence of abnormal grain growth. Induced by KSN, the KNN phase structure spontaneously transformed from perovskite to tetragonal tungsten bronze. The result suggested that for preparing KNN-based ceramics with high performance it is necessary to control the phase transformation. This study also opens up a new avenue for the investigation of the relationship between structure and performance in KNN ceramics.

INTRODUCTION

The attention on piezoelectric ceramics has been moving to Pb-free materials owing to increasing environmental and health concerns. Among Pb-free materials, $(K_{0.5}Na_{0.5})NbO_3$ (KNN)-based ceramics have been widely studied recently due to their high Curie temperature and good electrical properties [1, 2]. It is well known that pure KNN ceramics prepared by traditional sintering always lack sufficient density and high dielectric loss [3]. Various second phases have been used to prepare dense KNN-based ceramics with excellent performance [1, 2]. For example, an extremely high piezoelectric coefficient d_{33} of 570 pC/N was obtained by optimizing the composition [4]. Recently, Du's groups attained a large recoverable energy storage density of 4.08 J·cm⁻³ by the formation of $(K_{0.5}Na_{0.5})NbO_3$–$Bi(Me_{2/3}Nb_{1/3})O_3$ solid solutions (where Me^{2+} = Mg and Zn) [5]. Yang's group observed high transparency in $K_{0.5}Na_{0.5}NbO_3$–$Sr(Zn_{1/3}Nb_{2/3})O_3$ ceramics synthesized by conventional pressureless sintering [6]. Obviously, these reports provided a guideline on future research directions for the development of KNN ceramics. An effective method to improve the performance of KNN ceramics consist in by doping with a second phase.

Our recent study suggests that using of $KSr_2Nb_5O_{15}$ (KSN) particles prepared by a molten salt method promoted densification of ceramics during sintering [7, 8]. According to the literature, doping KNN with a small amount of Sr improved the density and electric properties of KNN [9, 10]. Marija *et al* [11] reported that a good transparency could be obtained due to the decrease of grain size in KNN–$SrTiO_3$ ceramics with increasing amounts of Sr. However, the composition cha- racteristics of $K_{0.5}Na_{0.5}NbO_3$–$KSr_2Nb_5O_{15}$ (KNN–KSN) ceramics have not yet been investigated so far. In this work, $KSr_2Nb_5O_{15}$ was used as a second phase. KNN––KSN ceramics were prepared by traditional sintering technology. Synthesis and composition characteristics of KNN–KSN ceramics were investigated.

EXPERIMENTAL

In the present study $(1–x)K_{0.5}Na_{0.5}NbO_3$–$xKSr_2Nb_5O_{15}$ ($(1 – x)KNN–xKSN$) ($x = 0$, 0.15, 0.30 and 0.45) ceramics were prepared by traditional solid-state reaction methods. KNN powder was fabricated by reactive sintering of K_2CO_3 (99 %), Na_2CO_3 (99 %) and Nb_2O_5 (99.6 %). These reagents were provided by Sinopharm Chemical Reagent Co., Ltd. (China). The raw materials were mixed homogeneously by ball milling in ethanol for 10 h using zirconia balls, then calcined in a temperature of 900°C for 4 h. The rates of heating and cooling were 5°C min⁻¹ and 2°C min⁻¹, respectively. KSN powder was prepared by a molten salt synthesis (MSS) method. Details of the synthesis of the KSN particles have been reported previously [12]. KNN, KSN powder and excess 2 mol. % Bi_2O_3 (99.9 %) were mixed by ball milling for 24 h with ethanol. After drying, the mixture was granulated with a binder of 6 wt. % poly vinyl alcohol (PVA) and then pressed into disk-shaped pellets with diameter 12 mm and thickness 1.3 mm. After burning off the PVA, all disk samples were sintered at 1050 ~ 1250°C or 2 h with a constant heating rate of 5°C·min⁻¹ and finally furnace-cooling to room temperature with a rate of 2°C·min⁻¹. Silver electrodes were coated on both surfaces of each sintered samples by firing at 600°C for 10 min.

Bulk densities of the sintered samples were determined by using the Archimedes method. The relative density was calculated based on the theoretical densities of KSN (5.002 g·cm^{-3}) and KNN (4.51 g·cm^{-3}). The phase structure of the KSN powder crystals and ceramics was characterized by X-ray diffraction (XRD, Panalytical X'Pert PRO, The Netherlands) using Cu Kα radiation and a graphite monochromator. Microstructures of the polished and thermally-etched disks were identified by scanning electron microscopy (SEM, Quanta 600 FEG, USA). The curves of the dielectric constant (ε) and dielectric loss (tan δ) against temperatures between 30°C to 500°C at 10 kHz, 100 kHz and 1 MHz were performed with an LCR precision electric bridge (Hewlett-Packard HP4284, Palo Alto, USA).

RESULTS AND DISCUSSION

Figure 1 shows the photographs of the (1 – *x*)KNN––*x*KSN ceramics (*x* = 0, 0.15, 0.30 and 0.45) prepared by sintering at temperatures in the range from 1050 to 1250°C. As shown in the figure, samples sintered at 1050°C did not exhibit any significant shrinkage. The KNN (without KSN) sample appeared bubbling phenomenon during heating up 1150°C and the large shrinkage occurred for 0.85KNN-0.15KSN sample. Heating to 1200°C resulted in further shrinkage for 0.7KNN-0.3KSN and 0.55KNN-0.45KSN samples. When the sintering temperature approached 1250°C, all samples showed overburning characteristics, such as bubbling and cracking. Obviously, the optimum sintering temperature for these samples was in the range from 1050°C to 1225°C. The temperature was increased with the increase of KSN content. Table 1 shows the density of the (1 – *x*)KNN–*x*KSN ceramics prepared at the optimized sintering temperature. The relative densities of the (1 – *x*)KNN–*x*KSN ceramics were greater than 90 %. The density increased and then decreased as a function of the KSN content, and reached a maximum value at *x* = 0.15. During the sintering stage, KSN grains consumed the surrounding smaller KNN grains and grew

competitively. A small amount of KSN promoted the ion diffusion due to the existence of vacancy defects [7, 8, 12]. Increasing KSN content casued that the large KSN grains impinged on one another and had less small grains to consume. This may be the reason for the occurrence of the optimal density in the 0.85KNN–0.15KSN ceramics. Thus, samples sintered at 1050°C, 1150°C, 1200°C and 1225°C for KNN–0KSN, 0.85KNN–0.15KSN, 0.70KNN–0.30KSN and 0.55KNN–0.45KSN, respectively, were used to examine the phase structure, microstructure and dielectric property.

Table 1. Density of the (1 – *x*)KNN–*x*KSN ceramics prepared at the optimized sintering temperature.

x	Sintering temperature (°C)	Density (g·cm^{-3})	Theoretical density (g·cm^{-3})	Relative density (%)
0	1050	4.245	4.51	94.12
0.15	1150	4.506	4.584	98.31
0.30	1200	4.397	4.658	94.41
0.45	1225	4.526	4.731	95.66

Figure 2 displays the XRD patterns of the (1 – *x*) KNN–*x*KSN ceramics (*x* = 0, 0.15, 0.30 and 0.45). A single phase was obtained for the sample in the case of *x* = 0. When x ≥ 0.15, a secondary phase was detected. The extra peaks could be indexed to the KSr$_2$Nb$_5$O$_{15}$ (JCPDF 34-0123) phase that exhibits tetragonal tungsten-bronze (TTB) type structure. An amplified zoom of the XRD profiles in the 2θ range from 31° to 33° is shown in the inset of Figure 2. It can be seen that the diffraction lines shifted toward larger 2θ angle with increasing KSN content (the position of the strongest peak of KSN being 32.136°). However, the peak did not exhibit splitting. This behavior could be related with the formation of a solid solution.

Figure 3 shows the evolution of the intensity ratio of KSN characteristic (410) peak to the strongest peak as a function of the KSN content. The value of this ratio significantly increased, suggesting that the addition of
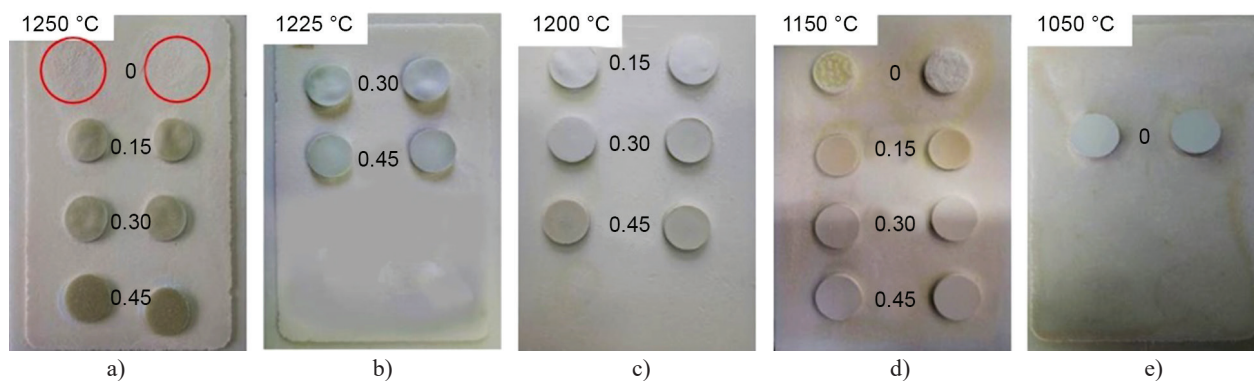

Figure 1. Photographs of the (1 – *x*)KNN–*x*KSN ceramics (*x* = 0, 0.15, 0.30 and 0.45).

KSN modified the crystalline structure. With the increase of KSN content, the crystal structure gradually changed from perovskite to TTB structure. In KNN ceramics, TTB secondary phase was usually formed owing to the volatilization of the potassium and sodium ions [1, 2]. The KNN phase also could be transformed easily from the TTB phase [13]. Therefore, our results suggested that K^+ and Na^+ had diffused into the KSN lattice to form a solid solution in the $(1-x)$KNN–xKSN ceramics.
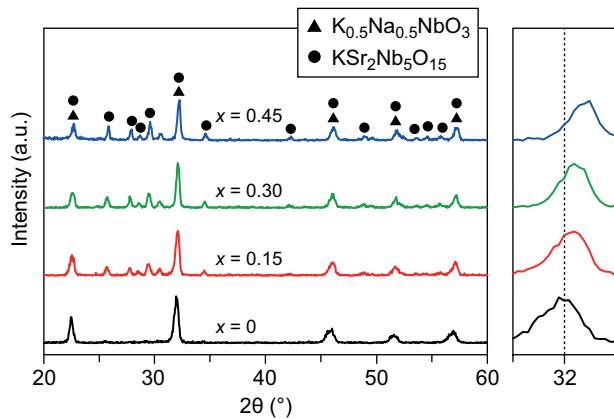

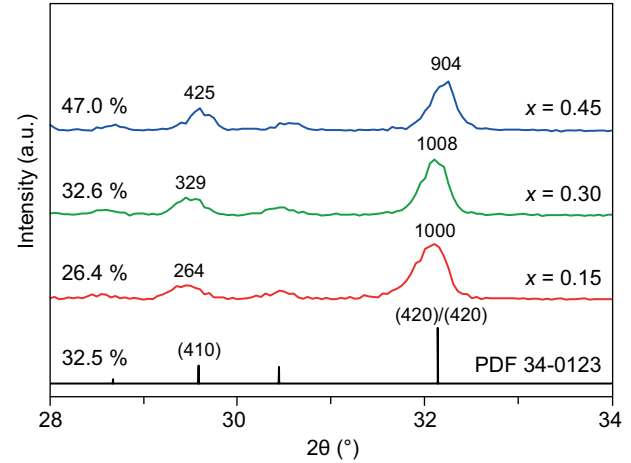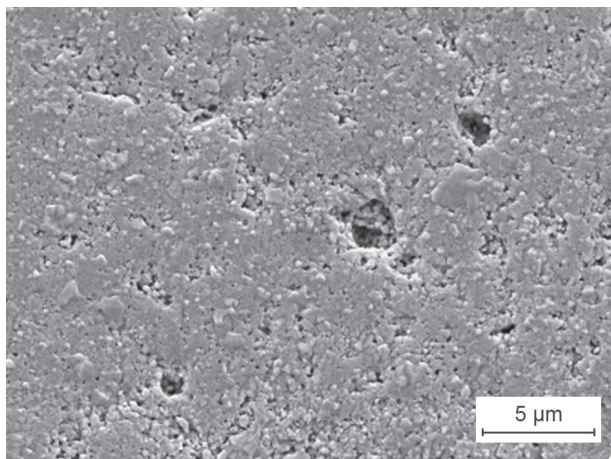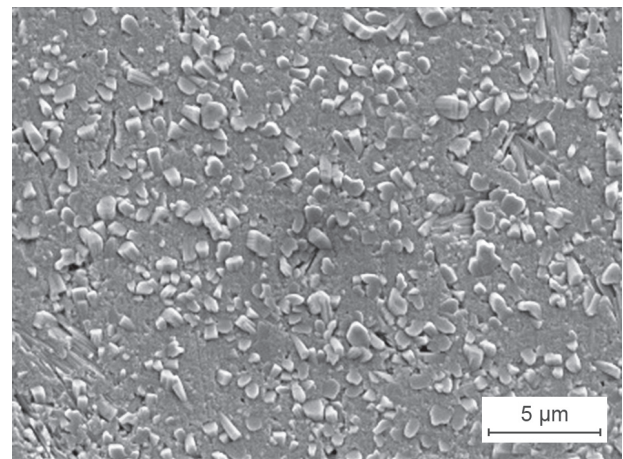Figure 2. XRD patterns of the $(1-x)$KNN–xKSN ceramics ($x = 0$, 0.15, 0.30 and 0.45).
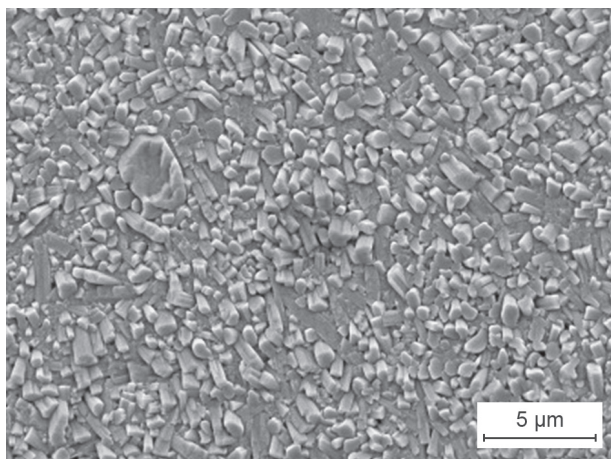

Figure 3. Magnified XRD patterns in the 28° – 34° region of the $(1-x)$KNN–xKSN ceramics.
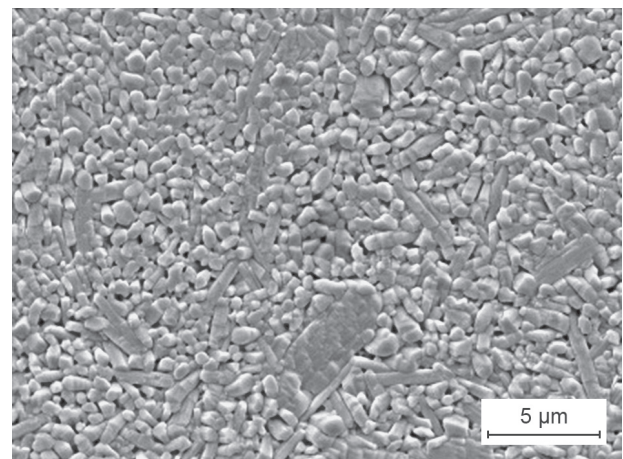

a) $x = 0$

b) $x = 0.15$

c) $x = 0.30$

d) $x = 0.45$

Figure 4. Microstructure of the $(1-x)$KNN–xKSN ceramics: a) $x = 0$, b) $x = 0.15$, c) $x = 0.30$ and d) $x = 0.45$.

The SEM images of the $(1 - x)$KNN–xKSN ceramics are shown in Figure 4. As seen in Figure 4a, the typical microstructures of the alkaline niobate ceramics are small and cubic equiaxed grains. A change of the microstructure was observed with KSN content as displayed in Figures 4b ~ d. As the KSN content increased, the percentage of columnar grain increased significantly. Furthermore, in the case of $x = 0.45$ the cube-like grains disappeared and only columnar grains remained. It was found that the columnar grain size was uniform for the case of $x = 0.45$ and almost the same with that of $x = 0.15$ and $x = 0.3$ (seen in Figures 4b and c) although the sintering temperature was the highest. Abnormal grain growth did not occur, contrary to what is often observed for other KNN-based ceramics [1, 2]. In other words, KSN particles inhibited the KNN grain growth. In addition, the porosity first decreased and then increased with increasing KSN content. This result suggested that a small amount of KSN particles promoted the density of KNN ceramics.

The assessment of phase structure needs more accurate measurement methods, and so the temperature dependence of dielectric constant was used to further confirm the phase structure. Figure 5 shows the temperature dependence of the dielectric constant (ε) and loss (tan δ) of the $(1 - x)$KNN–xKSN ceramics at different measuring frequencies (10 kHz, 100 kHz and 1 MHz). High dielectric losses were found for all samples over a wide temperature range (30°C to 500°C). This can be attributed to space charge effects due to doping with Bi₂O₃.

In order to investigate the effect of the KSN content, the measured frequency of 1MHz was chosen to remove space charge polarization contributions as shown in Figure 6. In the case of $x = 0$, the curve shows two anomalies. The anomaly at ~ 200°C was explained by the orthorhombic-tetragonal ($T_{\text{O-T}}$) phase transition, as well as a dielectric peak at ~ 400°C for the T_{C} (tetragonal-cubic phase transition). By comparison with that of pure KNN ceramics [1, 2], the broadening of the peaks suggests a diffuse phase transition. That is, the ceramics transformed gradually a "normal" to a diffuse phase transition when doping with Bi³⁺. Similar phenomena have appeared in Bi³⁺-doped KSN ceramics [7, 8]. This behavior could be attributed to an increase in the level of structural disorder due to the introduction of Bi³⁺ into the KNN structure and the subsequent occurrence of cationic vacancies. As seen in Figure 6, it is obvious that the addition of KSN decreased T_{C}, and $T_{\text{O-T}}$ disappeared T_{C} of the $(1 - x)$KNN–xKSN ceramics decreased gradual-
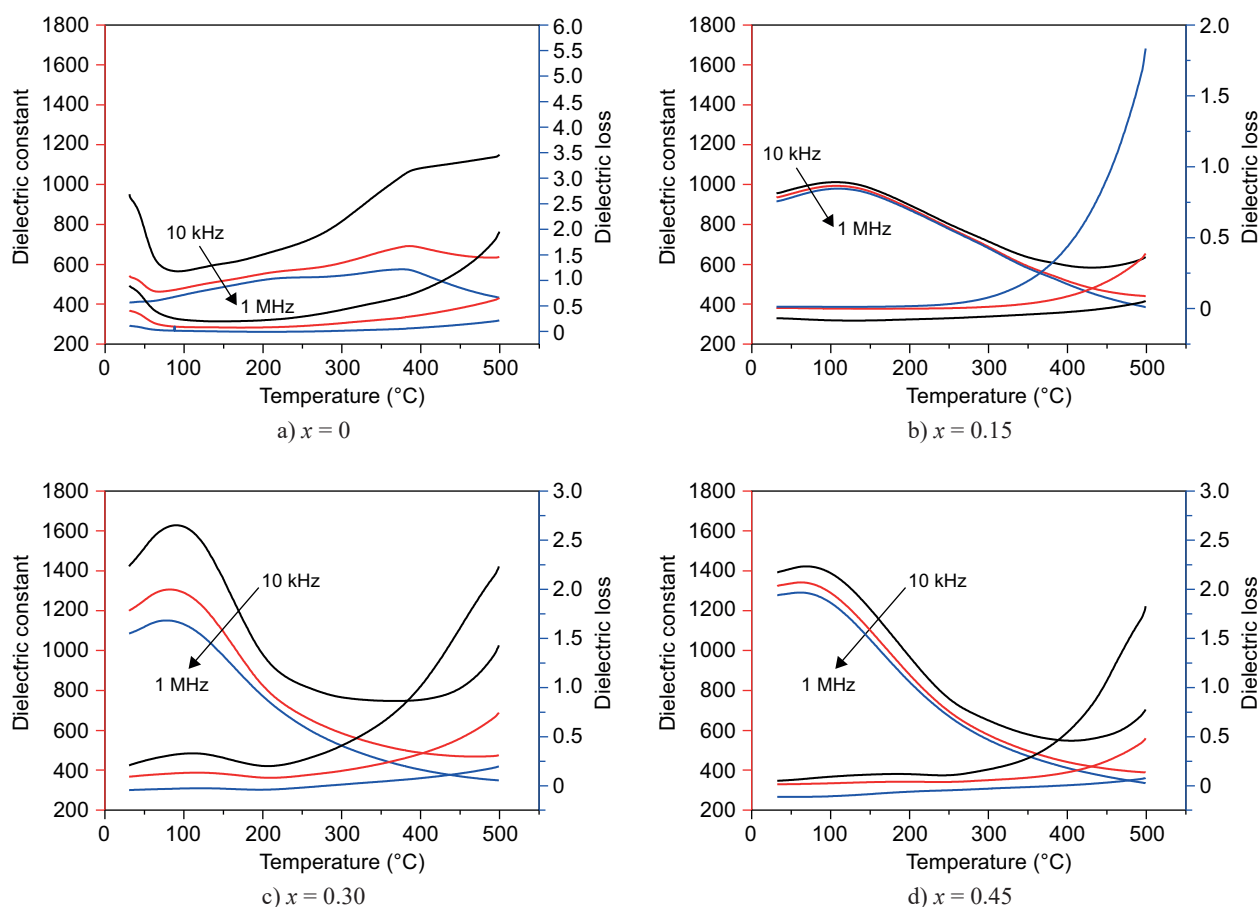

Figure 5. Temperature dependence of dielectric constant (ε) of the $(1 - x)$KNN–xKSN ceramics: a) $x = 0$, b) $x = 0.15$, c) $x = 0.30$ and d) $x = 0.45$.

ly with increasing KSN content. It should be noted that their T_C values were consistent with that of KSN ceramics. These results further confirmed the formation of a solid solution when adding with KSN into KNN. Generally, the dielectric properties are affected by the point defect concentration, especially oxygen vacancy, which is commonly found in electronic materials [14, 15]. As is well known, oxygen vacancies are involved in KNN ceramics owing to the volatilization of the alkali metal ions (K and Na) during high-temperature processing. So, more work needs to be done for understanding the influence of point defects, which will promote the development of excellent electrical properties in the KNN ceramics.
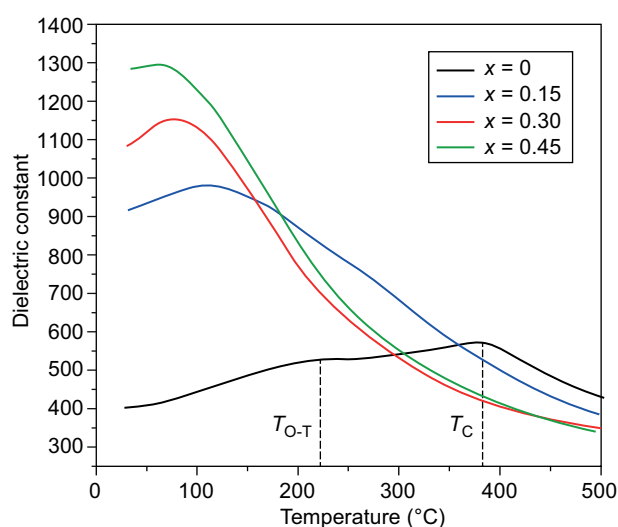

Figure 6. Temperature dependence of dielectric constant (ε) of the $(1 - x)$KNN–xKSN ceramics at 1 MHz.

CONCLUSIONS AND OUTLOOK

In this work, $(1 - x)$KNN–xKSN ceramics were designed to study the effect of KSN content on their sintering behavior and composition characteristics. The results showed that with the increase of KSN content, the sintering temperature of the $(1 - x)$KNN–xKSN ceramics increased and no abnormal grain growth (AGG) phenomenon was observed. This will give a guide to prepare dense KNN ceramics with uniform grain size by the conventional solid-state reaction method. It should be noted that a solid solution was formed due to the diffusion of K^+ and Na^+ into the KSN lattice. That is, the formation of TTB phase was promoted with the addition of KSN. This feature will be investigated in more detail in the future in order to obtain a better understanding of the relationship between structure and performance in KNN ceramics.

Acknowledgments

REFERENCES

1. Li J.F., Wang K., Zhu F.Y., Cheng L.Q., Yao F.Z. (2013): (K, Na)NbO₃-based lead-free piezoceramics: fundamental aspects, processing technologies, and remaining challenges. *Journal of the American Ceramic Society*, 96, 3677-3696. doi:10.1111/jace.12715

2. Zheng T., Wu J., Xiao D., Zhu J., Wang X., Lou X. (2015): Composition-driven phase boundary and piezoelectricity in potassium-sodium niobate-based ceramics. *ASC Applied Materials Interfaces*, 7, 20332-20341. doi: 10.1021/acsami.5b06033

3. Su Y.L., Chen X.M., Yu Z.D., Lian H.L., Zheng D.D., Peng J.H. (2017): Comparative study on microstructure and electrical properties of $(K_{0.5}Na_{0.5})NbO_3$ lead-free ceramics prepared via two different sintering methods. *Journal of Materials Science*, 52, 2934-2943. doi:10.1007/s1085

4. Xu K., Li J., Lv X., Wu J., Zhang X., Xiao D., Zhu J. (2016): Superior piezoelectric properties in potassium-sodium niobate lead-free ceramics. *Advanced Materials*, 28, 8519-8523. doi:10.1002/adma.201601859

5. Shao T., Du H., Ma H., Qu S., Wang J., Wang J., Wei X., Xu Z. (2017): Potassium-sodium niobate based lead-free ceramics: novel electrical energy storage materials. *Journal of Materials Chemistry A*, 5, 554-563. doi: 10.1039/C6TA07803F

6. Chai Q., Yang D., Zhao X., Chao X., Yang Z. (2017): Lead-free (K,Na)NbO₃-based ceramics with high optical transparency and large energy storage ability. *Journal of the American Ceramic Society*, doi: 10.1111/jace.15392

7. Liu L., Gao F., Zhang Y., Sun H. (2014): Dense KSr₂Nb₅O₁₅ ceramics with uniform grain size prepared by molten salt synthesis. *Journal of Alloys and Compounds*, 616, 293-299. doi: 10.1016/j.jallcom.2014.07.155

8. Liu L., Gao F., Hu G., Liu J., Li J. (2013): Microstructure and electrical properties of potassium strontium niobate (KSr₂Nb₅O₁₅) ceramics. *Journal of Alloys and Compounds*, 580, 93-100. doi: 10.1016/j.jallcom.2013.05.093

9. Malic B., Bernard J., Holc J., Kosec M. (2005): Strontium doped K₀.₅Na₀.₅NbO₃ based piezoceramics. *Ferroelectrics*, 314, 149-156. doi:10.1080/00150190590926373

10. Hrescak J., Drazic G., Deluca M., Arcon I., Kodre A., Dapiaggi M., Rojac T., Malic B., Bencan A. (2017): Donor doping of K₀.₅Na₀.₅NbO₃ ceramics with strontium and its implications to grain size, phase composition and crystal structure. *Journal of the European Ceramic Society*, 37, 2073-2082. doi: 10.1016/j.jeurceramsoc.2016.12.053

11. Marija K., Bobnar V., Hrovat M., Bernard J., Malic B., Holc J. (2004): New lead-free relaxors based on the K₀.₅Na₀.₅NbO₃––SrTiO₃ solid solution. *Journal of Materials Research*, 19, 1849-1854. doi: 10.1557/JMR.2004.0229

12. Liu L., Gao F., Hu G., Liu J., Li J. (2013): Effect of excess Nb₂O₅ on the growth behavior of KSr₂Nb₅O₁₅ particles by molten salt synthesis. *Powder Technology*, 235, 806-813. doi: 10.1016/j.powtec.2012.11.040

13. Luo L., Chen C., Luo H. (2015): The effects of precursors on the morphology and microstructure of potassium sodium niobate nanorods synthesized by molten salt synthesis. *CrystEngComm*, 17, 8710-8719. doi: 10.1039/C5CE01382H

14. Wu J., Xiao D., Zhu J. (2015): Potassium-sodium niobate lead-free piezoelectric materials: past, present, and future of phase boundaries. *Chemical Reviews*, 115, 2559-2595. doi: 10.1021/cr5006809

15. Liu Z.Q., Leusink D.P., Wang X., Lü W.M., Gopinadhan K., Annadi A., Zhao Y.L., Huang X.H., Zeng S.W., Huang Z., Srivastava A., Dhar S., Venkatesan T., Ariando (2011): Metal-insulator transition in SrTiO₃₋ₓ thin films induced by frozen-out carriers. *Physical Review Letters*, 107, 146-802. doi:10.1103/PhysRevLett.107.146802